Intraband and interband conductivity in systems of strongly interacting bosons

B. Grygiel, K. Patucha, and T. A. Zaleski
Institute of Low Temperature and Structure Research, Polish Academy of Sciences, Okólna 2, 50-422 Wroclaw, Poland
(Received 22 February 2017; revised manuscript received 31 July 2017; published 18 September 2017)

Motivated by recent experimental progress on measuring various correlation functions in systems of ultracold atoms in optical lattices, we study properties of the Bose-Hubbard model in external synthetic magnetic field to describe transport phenomena in a multiband strongly interacting bosonic systems. We calculate the conductivity both in the Mott insulator and superfluid phases and investigate its two main contributions: intra- and interband. It appears that the interband processes dominate the transport properties by at least an order of magnitude. Also, at finite temperatures, additional transport channels appear due to coupling of the thermally excited particles or holes to the external field.

DOI: 10.1103/PhysRevB.96.094520

I. INTRODUCTION

Recently, growing interest is devoted to measurements of correlation functions and nonequilibrum dynamics in ultracold atoms, which includes studies of transport phenomena in these systems. Experiments on the flow of atoms between engineered reservoirs with initial imbalance of particles allowed for verification of quantized conductance, as predicted by the Landauer theory, and for investigation of effects of disorder and temperature on the transport properties [1–9]. Addition of engineered gauge potentials, acting as a synthetic magnetic field [10–15], possibly allows for realization of steady states carrying a mass current in strongly correlated lattice systems [16], described by the Bose-Hubbard model (BHM). The advantage of ultracold gases that the particle density can be probed in real time with a single-site resolution [17–19] provides unprecedented possibility of measuring the transport properties of isolated quantum systems. One of the very recent practical examples is a scanning gate microscope, which allows for spatial mapping of the atomic flows with resolution up to 10 nm [20]. The technique was demonstrated to work for point contacts but can be generalized to any cold-atom system.

Studies of conductivity of strongly correlated systems of bosons have been performed both theoretically and analytically in various condensed-matter systems, e.g., superconductors [21], granular superconductors [22], or Josephson junction arrays [23–25]. Although ultracold atomic gases trapped in optical lattices are relatively small systems (with regard to number of particles), they still can be described using methods of solid-state physics [26]. In return, they allow for observation of many-body quantum effects not disturbed by lattice defects or material imperfections. The key phenomenon in these systems is a quantum phase transition between phase-coherent superfluid state (SF) and strongly localized Mott insulator (MI), which is tuned by strength of interactions between atoms [27], similar in many ways to the behavior of strongly correlated electronic systems, e.g., superconductors. As a result, they can provide a quantum simulation environment, in which the constituent particles behave similarly to electrons in solids. This leads to applicability of the same theoretical models (Bose-Hubbard or Hubbard models) and methods for both of them [26].

However, a full theoretical understanding of transport phenomena in strongly correlated lattice systems is still called for. Since, in the light of the recent experiments, accurate measurements of transport properties of atomic systems in strictly controlled, engineered environments are becoming possible, it is a goal of the present work to study the conductivity (a current-current correlation function) of the Bose-Hubbard model in the presence of artificial gauge potentials. This is realized by mapping the BHM to a quantum rotor model, which, including spatial correlation, allows for a proper description of particles occupying a multiband system resulting from the presence of the synthetic magnetic field.

The remainder of the paper is organized in the following way. Section II contains a brief overview of quantum rotor approximation to the Bose-Hubbard model and the calculations of the conductivity. For clarity, the calculations are divided into three parts: for intraband (Sec. II C 1) and interband components (Sec. II C 2) and for the superfluid component (Sec. II C 3). In the following section, the dependence of the conductivity on the frequency and the parameters of the model is presented. Section III B is focused on the influence of the temperature on the transport properties of the system. The paper is summarized in Sec. IV. In the appendix, details of the derivation of the expression for conductivity of multiband system are presented.

II. QUANTUM ROTOR APPROACH TO BOSE-HUBBARD MODEL

A. Hamiltonian

The simplest nontrivial model describing strongly interacting bosons in optical lattice is the Bose-Hubbard model [27,28]. The Hamiltonian written in the second quantization formalism reads

$$\hat{H} = -\sum_{\langle i,j\rangle} t_{ij}(\hat{a}_i^\dagger \hat{a}_j + \text{H.c.}) + \frac{U}{2}\sum_i \hat{n}_i^2 - \overline{\mu}\sum_i \hat{n}_i, \quad (1)$$

where $\hat{a}_i$ ($\hat{a}_i^\dagger$) is bosonic annihilation (creation) operator and $\hat{n}_i = \hat{a}_i^\dagger \hat{a}_i$ is the particle number operator at the lattice site i. The first term is related to hopping between the nearest neighboring sites with energy gain t_{ij}. The second one describes the repulsive interaction U between each two particles at the same lattice site. The last term is responsible for

controlling the number of bosons and includes $\overline{\mu} = \mu + U/2$, with μ being the chemical potential.

In the present paper, we consider a combination of the Bose-Hubbard model with the Harper model [29,30] to describe the transport properties of strongly interacting bosons in a synthetic magnetic field. Magnetic field enters the model through Peierls substitution, turning the hopping coefficient t into a complex number:

$$t_{ij} \to t \exp\left[\frac{2\pi i}{\Phi_0}\int_{\mathbf{r}_j}^{\mathbf{r}_i} \mathcal{A}(\mathbf{r})\cdot d\mathbf{l}\right], \tag{2}$$

where $\mathcal{A}(\mathbf{r})$ is the vector potential associated with the magnetic field and Φ_0 denotes the magnetic flux quantum. As we include only nearest neighbor hoppings, Eq. (2) reduces to $t_{ij} \to t\exp(2\pi i\alpha_{ij})$, where $2\pi\alpha_{ij}$ is the phase obtained by a particle moving from the site i to the site j. This operation changes the periodicity of the lattice, which now is governed by the periodicity of the phase factor. It leads to expansion of the elementary cell into the magnetic elementary cell and addition of basis to the lattice.

In the case of the square lattice, the kinetic part of Harper-Bose-Hubbard Hamiltonian (which equals simply to the Hamiltonian of the Harper model)

$$H_{\text{Harper}} = -t\sum_{\langle i,j\rangle}\left[e^{\frac{2\pi i}{\Phi_0}\int_{\mathbf{r}_j}^{\mathbf{r}_i}\mathcal{A}(\mathbf{r})\cdot d\mathbf{l}} a_i^\dagger(\tau)a_j(\tau) + \text{c.c.}\right] \tag{3}$$

can be expressed with use of the Fourier transform as

$$H_{\text{Harper}} = \frac{t}{N_e}\sum_{\mathbf{k}}[a_\mathbf{k}]^\dagger\mathcal{H}(\mathbf{k})[a_\mathbf{k}], \tag{4}$$

where $[a_\mathbf{k}]$ is a column vector of complex fields $a_\mathbf{k}^b$ for each site b (basis position) in the magnetic elementary cell, $[a_\mathbf{k}]^\dagger$ is its Hermitian conjugation, N_e denotes the number of the elementary cells, and $\mathcal{H}(\mathbf{k})$ is the kernel of the Harper Hamiltonian written in Landau gauge

$$\mathcal{H}(\mathbf{k}) = -\begin{bmatrix} D_1 & e^{ik_x} & 0 & \dots & e^{-ik_x} \\ e^{-ik_x} & D_2 & e^{ik_x} & \ddots & 0 \\ 0 & \ddots & \ddots & \ddots & \vdots \\ \vdots & \ddots & e^{-ik_x} & D_{q-1} & e^{ik_x} \\ e^{ik_x} & 0 & \dots & e^{-ik_x} & D_q \end{bmatrix} \tag{5}$$

with $D_q = 2\cos(k_y - 2\pi q\alpha)$. The strength of the field is given by the parameter $\alpha = \Phi/\Phi_0 = p/q$, which describes the ratio of the magnetic flux through elementary cell to the magnetic flux quantum. Numbers p and q are mutually prime integers while q is equal to the number of magnetic subbands, as well as the number of sites in the magnetic elementary cell. For irrational values of α, the dimension of the Harper matrix becomes infinite.

B. Method

In the following, we apply the quantum rotor approximation, in which the second-quantized Hamiltonian of the model is translated from the particle-number representation to a description in terms of the phase fields with the help of the path integral formalism [31]. This leads to an effective bosonic description of the strongly correlated system. The method is capable of handling spatial and quantum fluctuation effects properly in contrast to the mean-field approach, in which critical parameters are dependent only on the number of neighbors in the lattice but not on the lattice dimensionality. This makes the method well fitted for systems in engineered potentials, which change periodicity of the lattice and introduce complex tunneling elements in the BHM. The quantum rotor approach has been previously applied with success to describe quantum phase transitions [32], Josephson junction arrays [33], magnetic and superconducting system [34–36], phase transition in spin glasses [37], and phase transition of bosonic atoms in optical lattices [31,38,39].

In order to proceed, the path integral formulation with the Matsubara "imaginary time" $0 \leqslant \tau \leqslant \beta \equiv 1/k_BT$ (T being temperature) is introduced [40]. For simplicity, it is assumed that $\hbar = 1$. Application of coherent state representation allows us to write the BHM Hamiltonian in terms of complex fields $\overline{a}_i(\tau), a_i(\tau)$ [41]. While the Hamiltonian (1) retains its original form, the operators are substituted by the complex fields. The partition function in the path integral formalism reads

$$Z = \int [\mathcal{D}\overline{a}\mathcal{D}a]e^{-S[\overline{a},a]}, \tag{6}$$

with the action

$$S[\overline{a},a] = \int_0^\beta d\tau\left\{H[\overline{a}(\tau),a(\tau)] + \sum_i \overline{a}_i(\tau)\frac{\partial}{\partial\tau}a_i(\tau)\right\}, \tag{7}$$

where the additional part with summation over i is the Berry term. Next, we perform a gauge transformation of the complex fields

$$\begin{aligned} \overline{a}_i(\tau) &= e^{-i\phi_i(\tau)}\overline{b}_i(\tau), \\ a_i(\tau) &= e^{i\phi_i(\tau)}b_i(\tau), \end{aligned} \tag{8}$$

which allows us to separate them into the phase fields $\phi_i(\tau)$ [31,36,42,43] related to the U(1) phase symmetry naturally present in the Bose-Hubbard Hamiltonian and the "rotated" bosonic amplitudes $b_i(\tau)$, related to the superfluid density. As the phase transition between superfluid and Mott insulator is related to long-range phase ordering, the amplitude fields can be approximated $b_i(\tau) = b_0 + \delta b_i(\tau) \approx b_0$, while the phase $\phi_i(\tau)$ fluctuations are retained [31,38]. It is a reasonable since the system under consideration is a uniform system at sufficiently low temperatures and thus it is in a quasicoherent state. The effect of this assumption can also be observed in Ref. [21], where the shape phase diagram is determined mostly by the phase fluctuations. Nevertheless, the amplitude fluctuations can also be taken into account through the Bogoliubov method, which allows us, e.g., to obtain the momentum-resolved correlation functions [38]. The saddle-point value of b_0 minimizes the Hamiltonian in Eq. (1) and reads

$$b_0 = \sqrt{\frac{tz + \overline{\mu}}{U}}, \tag{9}$$

where z denotes the coordination number of the lattice. From the Eq. (9) it follows that this approach is valid only for finite values of t/U (specifically, for $U = 0$ the phase description

breaks down). Furthermore, the action in Eq. (7) is transformed into the action of interacting quantum rotors

$$S[\phi] = \int_0^\beta d\tau \left\{ -2J \sum_{\langle i,j \rangle} \cos(\phi_j - \phi_i + \alpha_{ij}) + \sum_i \left(\frac{\dot{\phi}_i^2}{2U} + i \frac{\overline{\mu}}{U} \dot{\phi}_i \right) \right\}, \tag{10}$$

with $J = t b_0^2$ and

$$Z = \int [\mathcal{D}\phi] e^{-S[\phi]}. \tag{11}$$

The phase variables ϕ are periodic with a period 2π and thus the path integral in Eq. (6) must be performed with the boundary condition $\phi_i(\beta) - \phi_i(0) = 2\pi l_i$ with $l_i = 0, \pm 1, \pm 2, \ldots$ [31].

Due to the gauge transformation of the fields $\overline{a}, a$ in Eq. (8), the superfluid order parameter $\Psi_B = \langle a_i(\tau) \rangle$ becomes a product of amplitude and phase components

$$\Psi_B = \langle b_i(\tau) \rangle \langle e^{i\phi_i(\tau)} \rangle = b_0 \psi_B, \tag{12}$$

where $\langle \cdots \rangle$ denotes statistical average. The consequence of the above factorization is that not only nonzero amplitude b_0 is required for the system to become superfluid but also the presence of the phase coherence resulting in a nonzero value of $\psi_B = \langle e^{i\phi_i(\tau)} \rangle$.

To proceed, unimodular fields $\zeta_i(\tau) = e^{i\phi_i(\tau)}$ are introduced using the following resolution of unity [38]:

$$1 = \int [\mathcal{D}\overline{\zeta} \mathcal{D}\zeta] \delta[\overline{\zeta}_i(\tau) - e^{-i\phi_i(\tau)}] \delta[\zeta_i(\tau) - e^{i\phi_i(\tau)}]. \tag{13}$$

The partition function in Eq. (6) can be calculated by relaxing the condition for the unimodularity of the fields $\overline{\zeta}, \zeta$ [35,44,45]. This is done by assuming that the fields are unimodular only on average:

$$|\zeta_i(\tau)|^2 = 1 \Rightarrow \frac{1}{N} \sum_i |\zeta_i(\tau)|^2 = 1. \tag{14}$$

Furthermore, the Dirac δ distribution can be represented using the Laplace transform $\delta(x) = \int d\lambda e^{\lambda x}$ to enforce the constraint (14). This procedure introduces a Lagrange multiplier λ. The partition function (11) can now be expanded into cumulant series up to terms quadratic in phase variables $\overline{\zeta}, \zeta$. After performing the Fourier transform into wave vector and Matsubara frequency domains, the partition function takes the form

$$Z = \int d\lambda \prod_{\mathbf{k},m} [d\overline{\zeta}_{\mathbf{k}}(\omega_m) d\zeta_{\mathbf{k}}(\omega_m)] e^{N\beta\lambda - S[\overline{\zeta},\zeta]}, \tag{15}$$

where the effective action of the interacting quantum rotors reads

$$S[\overline{\zeta},\zeta] = \frac{1}{\beta N} \sum_{m,\mathbf{k}} \overline{\zeta}_{\mathbf{k}}(\omega_m) \Gamma_\lambda^{-1}(\mathbf{k},\omega_m) \zeta_{\mathbf{k}}(\omega_m), \tag{16}$$

with the propagator

$$\Gamma_\lambda^{-1}(\mathbf{k},\omega_m) = \lambda + J\varepsilon_{\mathbf{k}} + \gamma_m^{-1}, \tag{17}$$

where $\omega_m = 2\pi m/\beta$ is the bosonic Matsubara frequency with $m = 0, \pm 1, \pm 2, \ldots$ and $\varepsilon_{\mathbf{k}}$ is a dispersion relation. For the simple square lattice $\varepsilon_{\mathbf{k}} = -2[\cos(k_x) + \cos(k_y)]$. However, in the presence of the synthetic magnetic field, it becomes more complicated and is given by eigenvalues of the Harper Hamiltonian kernel in Eq. (5), while Eq. (16) should include additional summation over magnetic subbands given by the dispersion relations, which here is omitted just for simplicity of presentation.

The propagator in Eq. (17) contains the phase-phase correlator function $\gamma(\tau - \tau') = \langle e^{i\phi(\mathbf{r},\tau) - i\phi(\mathbf{r},\tau')} \rangle$, which depends on a single site. The Fourier transform of the correlator in the limit of $\beta \to \infty$ takes form

$$\gamma_m^{-1} = \frac{U}{4} \left\{ 1 - 4 \left[v\left(\frac{\mu}{U}\right) + i \frac{\omega_m}{U} \right]^2 \right\}, \tag{18}$$

where $v(x) = x - \lfloor x \rfloor - 1/2$ and $\lfloor x \rfloor$ is the floor function, which returns the greatest integer less than or equal to x.

The spatial correlation function $\langle \overline{a}_{\mathbf{k}}(\omega_m) a_{\mathbf{k}}(\omega_m) \rangle$, required to determine the transport properties of the system, becomes factorized due to the gauge transformation (8) and reads

$$\langle \overline{a}_{\mathbf{k}}(\omega_m) a_{\mathbf{k}}(\omega_m) \rangle = b_0^2 \langle \overline{\zeta}_{\mathbf{k}}(\omega_m) \zeta_{\mathbf{k}}(\omega_m) \rangle \tag{19}$$

with the average $\langle \overline{\zeta}_{\mathbf{k}}(\omega_m) \zeta_{\mathbf{k}}(\omega_m) \rangle$ calculated from the partition function (15):

$$\langle \overline{\zeta}_{\mathbf{k}}(\omega_m) \zeta_{\mathbf{k}}(\omega_m) \rangle = N\beta \Gamma_\lambda(\mathbf{k},\omega_m). \tag{20}$$

In order to determine the Lagrange multiplier λ, the saddle-point method in the thermodynamic limit ($N \to \infty$) can be employed

$$\left. \frac{\partial S}{\partial \lambda} \right|_{\lambda = \lambda_0} = 0 \tag{21}$$

with the stationary point value of λ_0. This leads to the equation of state:

$$1 - \psi_B^2 = \langle \overline{\zeta}_i(\tau) \zeta_i(\tau) \rangle = \frac{1}{N\beta} \sum_{\mathbf{k},m} \Gamma_{\lambda_0}(\mathbf{k},\omega_m). \tag{22}$$

At the critical point, the Lagrange multiplier is given by the condition:

$$\Gamma_{\lambda_{0c}}^{-1}(\mathbf{k} = 0, \omega_m = 0) = 0 \;\Rightarrow\; \lambda_{0c} = -J\varepsilon_0 - \gamma_0^{-1}, \tag{23}$$

which is equivalent to the divergence of the order parameter susceptibility at the phase transition. It is worth noticing that in the ordered phase, the Lagrange multiplier stays constant and equal to the value at the critical point (λ_{0c}). In the disordered state, the Lagrange multiplier has to be calculated directly from Eq. (22) with ψ_B set to zero. Inserting the value of λ_{0c} into the equation of state (22), performing the summation over Matsubara frequencies, and introducing the lattice density of states (DOS),

$$\rho(x) = \frac{1}{N} \sum_{\mathbf{k}} \delta(x - \varepsilon_{\mathbf{k}}), \tag{24}$$

yields the equation of state in the form

$$1 - \psi_B^2 = \frac{1}{4} \int_{-\infty}^{\infty} dx \, \frac{\rho(x)[f_+(\beta,\Xi) + f_-(\beta,\Xi)]}{\Xi}, \tag{25}$$

where

$$\Xi = \sqrt{\frac{J}{U}(x-\varepsilon_0) + \frac{\delta\lambda}{U} + v^2\left(\frac{\mu}{U}\right)}. \tag{26}$$

and $\delta\lambda$ is a difference between the values of the Lagrange multiplier calculated in the Mott phase from Eq. (25) and in the superfluid state $\delta\lambda = \lambda_0 - \lambda_{0c}$. The function $1/\Xi(x)$ is related to the ground-state distribution of bosons over single-particle states with dimensionless energy x, while the expressions

$$f_\pm(\beta,\Xi) = \coth\left\{\frac{U\beta}{2}\left[\Xi \pm v\left(\frac{\mu}{U}\right)\right]\right\} \tag{27}$$

give the thermal distribution of the quasiholes (+) and quasiparticles (−).

The density of states function $\rho(x)$ in Eq. (24) encodes lattice geometry (also for lattices with basis) and possible quantum phase change resulting from particle movement through the lattice. As a result, the effects of the synthetic magnetic field are contained in the shape of $\rho(x)$, allowing us to obtain expressions for various observables in general form. However, it should be noted that it may be required to take into account a multiband character of $\rho(x)$ (e.g., for lattices with basis), as is in the case of the systems in the synthetic magnetic field.

C. Conductivity

The conductivity of the system can be calculated using linear response theory:

$$\sigma_{ij}(\omega_\nu) = -\frac{1}{N\beta\omega_\nu}\int_0^\beta d\tau d\tau' \frac{\delta^2 \ln Z}{\delta A_j(\tau')\delta A_i(\tau)}\bigg|_{\mathbf{A}=0} e^{i\omega_\nu(\tau'-\tau)}, \tag{28}$$

where $\mathbf{A}(\mathbf{r},\tau)$ is an external probe field assumed to be uniform in space and $N = N_e N_b$ with N_b denoting the number of sites in the elementary cell [21,46–48].The partition function can be written in the form $Z = \int[\mathcal{D}\bar{a}\mathcal{D}a]\exp[-(S_A + S')]$, where the action S_A after Fourier transform reads

$$S_A = \frac{t}{N_e}\int_0^\beta d\tau \sum_{\mathbf{k}} [a_{\mathbf{k}}]^\dagger \mathcal{H}\left(\mathbf{k} - \frac{2\pi}{\Phi_0}\mathbf{A}\right)[a_{\mathbf{k}}], \tag{29}$$

and S' contains the remaining terms of the action. The matrix $\mathcal{H}(\mathbf{k} - \frac{2\pi}{\Phi_0}\mathbf{A})$ denotes an arbitrary Hamiltonian kernel, which in our case is equal to the Harper Hamiltonian kernel defined in Eq. (5).

Inserting the action (29) into the formula (28), performing the Fourier transform to Matsubara frequency domain, and using Wick's theorem lead to a general formula for the conductivity of a system with multiple bands:

$$\begin{aligned}\sigma_{ij}(\omega_\nu) = &-\frac{1}{N\beta^3\omega_\nu}\left(\frac{2\pi t}{\Phi_0 N_e}\right)^2 \sum_{m,\mathbf{k}}\sum_{c,d,e,f}\frac{\partial\mathcal{H}_{cd}(\mathbf{k})}{\partial k_i}\frac{\partial\mathcal{H}_{ef}(\mathbf{k})}{\partial k_j}\\ &\times\left\langle\bar{a}^c_{\mathbf{k}}(\omega_m)a^f_{\mathbf{k}}(\omega_m)\right\rangle\left\langle\bar{a}^e_{\mathbf{k}}(\omega_{\nu+m})a^d_{\mathbf{k}}(\omega_{\nu+m})\right\rangle\\ &+\frac{1}{N\beta^2\omega_\nu}\left(\frac{2\pi}{\Phi_0}\right)^2\frac{t}{N_e}\sum_{m,\mathbf{k}}\sum_{c,d}\frac{\partial^2\mathcal{H}_{cd}(\mathbf{k})}{\partial k_i\partial k_j}\\ &\times\left\langle\bar{a}^c_{\mathbf{k}}(\omega_m)a^d_{\mathbf{k}}(\omega_m)\right\rangle,\end{aligned} \tag{30}$$

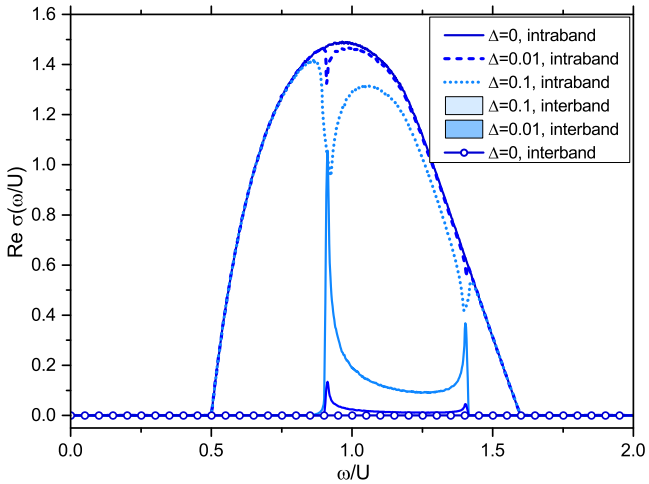

FIG. 1. The conductivity calculated for a square lattice in staggered potential. The offset energy Δ was added in order to differentiate between neighboring sites. For $\Delta = 0$ there is only intraband contribution to the conductivity. The interband channel appears only for nonzero Δ and its value increases with increasing Δ.

where the first term is called "paramagnetic" and the second is "diamagnetic" [21,24]. The averages $\langle\cdots\rangle$ are calculated with the partition function Z defined in (6) and are diagonal in wave vector $\mathbf{k}$ and Matsubara frequencies ω_m. Indices c, d, e, and f run over the positions in the elementary cell $1\ldots N_b$ (over the elements of the lattice basis). The derivatives over wave vectors have been introduced instead of the functional derivatives over vector potentials as the Hamiltonian kernel $\mathcal{H}$ depends on $\mathbf{k}$ in the same manner as on $\mathbf{A}$:

$$\frac{\delta\mathcal{H}_{ab}\left[\mathbf{k} - \frac{2\pi}{\Phi_0}\mathbf{A}(\tau')\right]}{\delta A_i(\tau)} = -\frac{2\pi}{\Phi_0}\delta(\tau-\tau')\frac{\partial\mathcal{H}_{ab}\left[\mathbf{k} - \frac{2\pi}{\Phi_0}\mathbf{A}(\tau')\right]}{\partial k_i}. \tag{31}$$

The kernel of the Hamiltonian can be decomposed using unitary matrix $\mathcal{U}$, which diagonalizes it, taking the form

$$\mathcal{H} = \mathcal{U}\mathcal{E}\mathcal{U}^{-1}, \tag{32}$$

where $\mathcal{E}$ is a diagonal matrix of eigenvalues of the matrix $\mathcal{H}$. This allows us to write the averages $\langle\bar{a}^a_{\mathbf{k}}(\omega_m)a^c_{\mathbf{k}}(\omega_m)\rangle$ in Eq. (30) as

$$\begin{aligned}\left\langle\bar{a}^a_{\mathbf{k}}(\omega_m)a^c_{\mathbf{k}}(\omega_m)\right\rangle &= |b_0|^2\left\langle\bar{\zeta}^a_{\mathbf{k}}(\omega_m)\zeta^c_{\mathbf{k}}(\omega_m)\right\rangle\\ &= N_e\beta|b_0|^2\sum_b \mathcal{U}_{cb}\Gamma_b(\mathbf{k},\omega_m)(\mathcal{U}^{-1})_{ba},\end{aligned} \tag{33}$$

with $\Gamma_b^{-1}(\mathbf{k},\omega_m) = J\mathcal{E}_b(\mathbf{k}) + \lambda + \gamma_m^{-1}$ being the propagator defined in (17).

Using the properties of the unitary matrix $\mathcal{U}$, one can arrive at the formula for the conductivity that separates intra- and interband contributions to the particle transport:

$$\sigma_{ij}(\omega_\nu) = \sigma_{ij}^{\text{intra}}(\omega_\nu) + \sigma_{ij}^{\text{inter}}(\omega_\nu). \tag{34}$$

The distinction between intra- and interband parts is important, since the latter occurs only in the systems with lattice basis. This effect is illustrated in Fig. 1, where the conductivity of the simple square (2D) lattice has been presented. To introduce a lattice basis, an offset energy Δ has been added

to every-second lattice site in the x direction, forming a staggered potential. For $\Delta = 0$ (no lattice basis) only the intraband conductivity is present. For nonzero values of Δ, the interband channel appears and as the parameter Δ grows, the contribution of the interband part to the conductivity increases. As a result, band splitting, introduced here by different onsite energies (alternatively also by the presence of the synthetic magnetic field), allows for additional transitions, absent in simple lattices. The in-depth derivation of formula (34) is relegated to the appendix.

1. Intraband conductivity

The intraband part of conductivity takes the form

$$\sigma_{ij}^{\mathrm{intra}}(\omega_\nu) = -\frac{1}{N\beta\omega_\nu}\left(\frac{2\pi J}{\Phi_0}\right)^2 \sum_{\mathbf{k},m,b} \frac{\partial\mathcal{E}_b(\mathbf{k})}{\partial k_j}\frac{\partial\mathcal{E}_b(\mathbf{k})}{\partial k_i} \times \{\Gamma_b(\mathbf{k},\omega_m)\Gamma_b(\mathbf{k},\omega_{m+\nu}) - [\Gamma_b(\mathbf{k},\omega_m)]^2\}. \quad (35)$$

The next steps in calculations are the summation over Matsubara frequencies $\omega_m = 2\pi m/\beta$, followed by the analytical continuation to real frequencies $\omega_\nu = \epsilon - i\omega$ with $\epsilon \to 0^+$. At this point, $\sigma_{ij}^{\mathrm{intra}}(\omega)$ can be split into two parts: singular and regular. The singular part

$$\mathrm{Re}\,\sigma_{ij,\mathrm{sing}}^{\mathrm{intra}}(\omega) = \frac{\beta\pi^3 J^2}{4\Phi_0^2}\sum_b \int dx\, \delta(\omega)\varrho_b^{ij}(x) \times \frac{\mathrm{csch}^2\left\{\frac{U\beta}{2}\left[\Xi_b - v\left(\frac{\mu}{U}\right)\right]\right\} + \mathrm{csch}^2\left\{\frac{U\beta}{2}\left[\Xi_b + v\left(\frac{\mu}{U}\right)\right]\right\}}{\Xi_b^2} \quad (36)$$

is the standard Drude conductivity, which exhibits a δ-like peak at $\omega = 0$ for nonzero temperatures. The peak is present even in the insulator phase due to nondissipative nature of the considered system [24,25]. The $\varrho_b^{ij}(x)$ in Eq. (36) stands for the generalized density of states (GDOS) for each band and is defined as

$$\varrho_b^{ij}(x) = \frac{1}{N}\sum_{\mathbf{k}} \frac{\partial\mathcal{E}_b(\mathbf{k})}{\partial k_i}\frac{\partial\mathcal{E}_b(\mathbf{k})}{\partial k_j}\delta[x - \mathcal{E}_b(\mathbf{k})], \quad (37)$$

and the quantity Ξ_b^2 is the analog of the function introduced in Eq. (26), but is defined for a single band (instead of all bands), which is reflected in the presence of the dispersion relation of that band $\mathcal{E}_b(\mathbf{k})$,

$$\Xi_b^2 = \frac{J}{U}[\mathcal{E}_b(\mathbf{k}) - E_0] + \frac{\delta\lambda}{U} + v^2\left(\frac{\mu}{U}\right), \quad (38)$$

with E_0 being the edge of the lowest band. The regular part of the conductivity takes the following form:

$$\mathrm{Re}\,\sigma_{ij,\mathrm{reg}}^{\mathrm{intra}}(\omega) = \frac{\pi^3}{\Phi_0^2}\left(\frac{J}{U}\right)^2 \sum_b \int dx\, \varrho_b^{ij}(x)\delta\left(\frac{\omega^2}{U^2} - 4\Xi_b^2\right) \times \frac{f_+(\beta,\Xi_b) + f_-(\beta,\Xi_b)}{\Xi_b^2}, \quad (39)$$

where $f_\pm(\beta,\Xi_b)$ are the thermal distributions of the quasiparticles (holes and particles, respectively), defined earlier, in Eq. (27).

In the zero-temperature limit, the intraband conductivity simplifies to the following form:

$$\mathrm{Re}\,\sigma_{ij,\mathrm{reg}}^{\mathrm{intra}}(\omega)\Big|_{T\to 0} = \frac{2\pi^3}{\Phi_0^2}\frac{J}{U}\frac{\varrho^{ij}\left[E_0 - \frac{\delta\lambda}{J} - \frac{v^2(\mu/U)}{J/U} + \frac{(\omega/U)^2}{4J/U}\right]}{(\omega/U)^2}, \quad (40)$$

where

$$\varrho^{ij}(x) = \sum_b \varrho_b^{ij}(x). \quad (41)$$

The form of the generalized density of states (37) suggests that there is no transverse contribution to the intraband conductivity: Because of the parity of the dispersion relation, the derivatives $\partial\mathcal{E}(\mathbf{k})/\partial k_i$ for $\mathbf{k}$ and $-\mathbf{k}$ cancel each other. As a result, the intraband conductivity (35) for $i \neq j$ vanishes.

2. Interband conductivity

The interband conductivity takes following form:

$$\sigma_{ij}^{\mathrm{inter}}(\omega_\nu) = -\frac{1}{N\beta\omega_\nu}\left(\frac{2\pi J}{\Phi_0}\right)^2 \sum_{\mathbf{k},m,b\neq b'} M_{bb'}^{ij}(\mathbf{k}) \times [\Gamma_b(\mathbf{k},\omega_m)\Gamma_{b'}(\mathbf{k},\omega_{m+\nu}) - \Gamma_b(\mathbf{k},\omega_m)\Gamma_{b'}(\mathbf{k},\omega_m)]. \quad (42)$$

The quantity $M_{bb'}^{ij}(\mathbf{k})$ is an equivalent of the weight $[\partial\mathcal{E}_b(\mathbf{k})/\partial k_j\ \partial\mathcal{E}_b(\mathbf{k})/\partial k_i]$ in the intraband part of conductivity in Eq. (35) and is defined as

$$M_{bb'}^{ij}(\mathbf{k}) = \sum_{c,c',d,d'} (\mathcal{U}^{-1})_{bc}\frac{\partial\mathcal{H}_{cd}}{\partial k_j}\mathcal{U}_{db'}(\mathcal{U}^{-1})_{b'c'}\frac{\partial\mathcal{H}_{c'd'}}{\partial k_i}\mathcal{U}_{d'b}, \quad (43)$$

which using bra-ket notation can be rewritten as

$$M_{bb'}^{ij}(\mathbf{k}) = \left\langle b\left|\frac{\partial\mathcal{H}}{\partial k_j}\right|b'\right\rangle\left\langle b'\left|\frac{\partial\mathcal{H}}{\partial k_i}\right|b\right\rangle, \quad (44)$$

where $|b\rangle$ is an eigenvector of $\mathcal{H}$.

The form of the interband part of the conductivity [specifically, the presence of $M_{bb'}^{ij}(\mathbf{k})$] does not allow introduction of the generalized density of states. As a result, replacing the summation over the Brillouin zone with easier integration over the energy domain is not possible.

By defining

$$\Omega_{bb'}(\mathbf{k},\omega_\nu) = \sum_m \frac{\Gamma_b(\mathbf{k},\omega_m)\Gamma_{b'}(\mathbf{k},\omega_{m+\nu}) - \Gamma_b(\mathbf{k},\omega_m)\Gamma_{b'}(\mathbf{k},\omega_m)}{\omega_\nu}, \quad (45)$$

the real part of the interband conductivity can be written as

$$\begin{aligned}\mathrm{Re}\,\sigma_{ij}^{\mathrm{inter}}(\omega_\nu) = -\frac{1}{N\beta}\left(\frac{2\pi J}{\Phi_0}\right)^2 \sum_{\mathbf{k}}\sum_{b\neq b'} \\ \times\left[\mathrm{Re}\,M_{bb'}^{ij}(\mathbf{k})\mathrm{Re}\,\Omega_{bb'}(\mathbf{k},\omega_\nu)\right. \\ \left.+\mathrm{Im}\,M_{bb'}^{ij}(\mathbf{k})\mathrm{Im}\,\Omega_{bb'}(\mathbf{k},\omega_\nu)\right]. \quad (46)\end{aligned}$$

To proceed, we can restrict ourselves to the case of longitudinal conductivity, i.e., $i = j$. From the definition in Eq. (44), the weight for $i = j$ reads

$$M_{bb'}^{ii}(\mathbf{k}) = \left\langle b\left|\frac{\partial\mathcal{H}}{\partial k_i}\right|b'\right\rangle\left\langle b'\left|\frac{\partial\mathcal{H}}{\partial k_i}\right|b\right\rangle = \left|\left\langle b\left|\frac{\partial\mathcal{H}}{\partial k_i}\right|b'\right\rangle\right|^2, \quad (47)$$

which is always real, so the imaginary part of $M_{bb'}^{ij}(\mathbf{k})$ zeros for $i = j$. As a result, we obtain

$$\begin{aligned}\mathrm{Re}\,\sigma_{ii}^{\mathrm{inter}}(\omega_\nu) = -\frac{1}{N\beta}\left(\frac{2\pi J}{\Phi_0}\right)^2 \sum_{\mathbf{k}}\sum_{b\neq b'}\mathrm{Re}\,M_{bb'}^{ii}(\mathbf{k}) \\ \times\,\mathrm{Re}\,\Omega_{bb'}(\mathbf{k},\omega_\nu). \quad (48)\end{aligned}$$

The summation over Matsubara frequencies in the term $\mathrm{Re}\,\Omega_{bb'}(\mathbf{k},\omega_\nu)$ and the analytical continuation to the real frequencies can be performed as in Sec. II C 1. By restricting the frequency domain to the positive frequencies only, i.e., $\omega > 0$, one obtains the final formula for the longitudinal interband conductivity:

$$\begin{aligned}&\mathrm{Re}\,\sigma_{ii}^{\mathrm{inter}}(\omega > 0) \\ &= \frac{\pi^3 J^2}{2N\Phi_0^2U^2}\sum_{\mathbf{k}}\sum_{b\neq b'}\mathrm{Re}\,M_{bb'}^{ii}(\mathbf{k}) \\ &\times\left\{\frac{f_+(\beta,\Xi_b)+f_-(\beta,\Xi_{b'})}{\Xi_b\Xi_{b'}\frac{\omega}{U}}\delta\left[\frac{\omega}{U}-(\Xi_b+\Xi_{b'})\right]\right. \\ &+\frac{f_-(\beta,\Xi_b)-f_-(\beta,\Xi_{b'})}{\Xi_b\Xi_{b'}\frac{\omega}{U}}\delta\left[\frac{\omega}{U}-(\Xi_{b'}-\Xi_b)\right] \\ &\left.-\frac{f_+(\beta,\Xi_b)-f_+(\beta,\Xi_{b'})}{\Xi_b\Xi_{b'}\frac{\omega}{U}}\delta\left[\frac{\omega}{U}-(\Xi_b-\Xi_{b'})\right]\right\}. \quad (49)\end{aligned}$$

The first term refers to the excitation of a particle-hole pair by the external field. The second one does not vanish only in nonzero temperatures and describes the thermal excitation of particles to higher bands. Similarly, the third term refers to thermally excited holes.

3. Superfluid part

The superfluid part of the conductivity can be recovered from the Eq. (30) for the intraband case. One can extract a term containing the order parameter from the diamagnetic term

$$\begin{aligned}\sigma_{ij}(\omega_\nu) = -\frac{1}{N\beta^3\omega_\nu}\left(\frac{2\pi t}{\Phi_0^2N_e}\right)^2\sum_{m,\mathbf{k},b}\frac{\partial\mathcal{E}_b(\mathbf{k})}{\partial k_i}\frac{\partial\mathcal{E}_b(\mathbf{k})}{\partial k_j} \\ \times\left\langle\overline{a}_{\mathbf{k}}^b(\omega_m)a_{\mathbf{k}}^b(\omega_m)\right\rangle\left\langle\overline{a}_{\mathbf{k}}^b(\omega_{\nu+m})a_{\mathbf{k}}^b(\omega_{\nu+m})\right\rangle \\ +\frac{1}{N\beta^2\omega_\nu}\left(\frac{2\pi}{\Phi_0}\right)^2\frac{t}{N_e}\sum_{m,\mathbf{k},b}{}'\frac{\partial^2\mathcal{E}_b(\mathbf{k})}{\partial k_i\partial k_j} \\ \times\left\langle\overline{a}_{\mathbf{k}}^b(\omega_m)a_{\mathbf{k}}^b(\omega_m)\right\rangle \\ +\frac{1}{N\beta^2\omega_\nu}\left(\frac{2\pi}{\Phi_0}\right)^2\frac{t}{N_e}\left.\frac{\partial^2\mathcal{E}_1(\mathbf{k})}{\partial k_i\partial k_j}\right|_{\mathbf{k}=0} \\ \times\left\langle\overline{a}_0^1(\omega_0)a_0^1(\omega_0)\right\rangle, \quad (50)\end{aligned}$$

where the summation denoted with the prime ($\sum'$) is performed over all states except the state with $\mathbf{k} = 0$, $\omega_m = \omega_0 = 0$ in the lowest band ($b = 1$), which is related to the order parameter in the following way:

$$\Psi_B^2 = \frac{1}{NN_e\beta^2}\left\langle\overline{a}_0^1(\omega_0)a_0^1(\omega_0)\right\rangle. \quad (51)$$

Taking into account the relation between the superfluid order parameter and phase coherence order parameter in Eq. (12) and the fact that for $i \neq j$ the second derivative of the lowest band dispersion vanishes, the last line in Eq. (50) can be identified as a contribution to conductivity resulting from presence of the superfluid state:

$$\sigma_{ii}^{SF}(\omega_\nu) = \frac{J}{\omega_\nu}\left(\frac{2\pi}{\Phi_0}\right)^2\left.\frac{\partial^2\mathcal{E}_1(\mathbf{k})}{\partial k_i^2}\right|_{\mathbf{k}=0}\psi_B^2. \quad (52)$$

Similarly to the previous calculation, the analytical continuation to the real frequencies must be performed and the dependence of the superfluid conductivity on frequency reads

$$\begin{aligned}\sigma_{ii}^{SF}(\omega) = \frac{4\pi^3 J}{\Phi_0^2}\left.\frac{\partial^2\mathcal{E}_1(\mathbf{k})}{\partial k_i^2}\right|_{\mathbf{k}=0}\psi_B^2\delta(\omega) \\ +i\frac{4\pi^2 J}{\Phi_0^2}\left.\frac{\partial^2\mathcal{E}_1(\mathbf{k})}{\partial k_i^2}\right|_{\mathbf{k}=0}\frac{\psi_B^2}{\omega}, \quad (53)\end{aligned}$$

which is in agreement with previous results [21,24].

III. LONGITUDINAL INTRA- AND INTERBAND CONDUCTIVITY

A. Zero-temperature limit

In this section, we analyze the behavior of both intra- and interband conductivity with varying model parameters, i.e., hopping energy, chemical potential, and temperature.

In our approach, in order to observe the SF-MI phase transition in nonzero temperature, the system needs to be in the three-dimensional universality class (in agreement with the Mermin-Wagner theorem [49]). To this end, we use a cubic lattice with a very small ($10^{-4}t$) interlayer coupling in the z direction, making the system quasi-two-dimensional, but still exhibiting a bulk phase transition. The synthetic magnetic field breaks the lattice translational symmetry. In order to restore it, the introduction of a magnetic supercell is required. This immediately leads to splitting of the band structure. The obtained energy structure for a square lattice is represented by the famous Hofstadter butterfly [30], which is a solution of the Harper's equation [29].

In order to represent the effects of the synthetic magnetic field in the form of the lattice density of states or lattice dispersion relation, Harper's equation needs to be diagonalized. As it becomes more difficult and time-consuming for larger numbers of energy bands, here we present the results only for a few

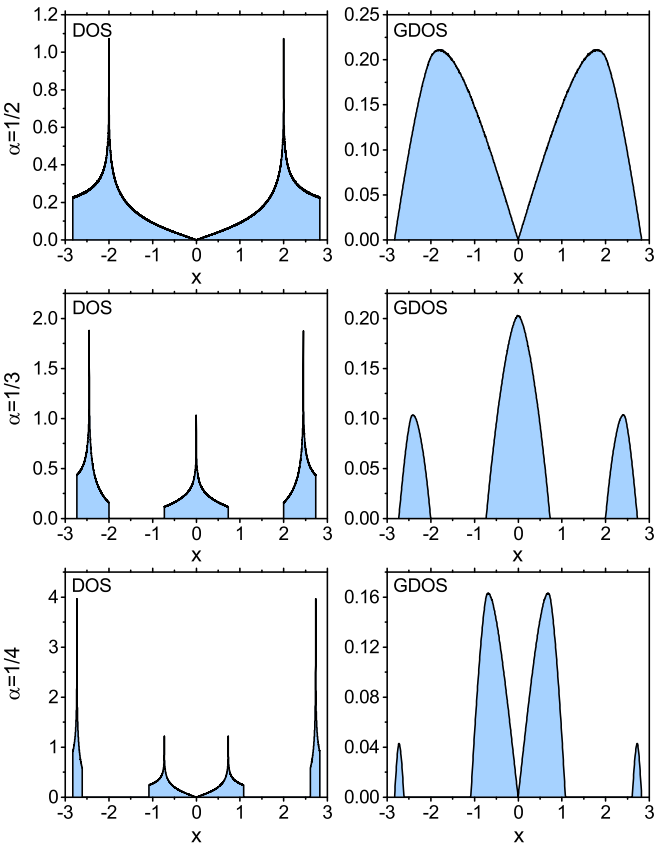

FIG. 2. Densities of states and generalized densities of states for three values of the magnetic field given by the parameter α.

values of the magnetic flux α corresponding to strong fields, $\alpha = 1/2,\ 1/3,\ 1/4$. A case of $\alpha = 1/2$ for bosonic atoms in optical lattice has been already achieved experimentally [50].

The magnetic DOS and respective generalized DOS for the considered cases are presented in Fig. 2. The DOS and GDOS reflect the splitting of the energy structure into q bands for $\alpha = 1/q$. For the interband conductivity, the role of GDOS is taken over by $M^{xx}_{bb'}(\mathbf{k})$, which is defined for each pair of bands, as presented in Fig. 3 for three-band case ($\alpha = 1/3$). The phase diagrams, derived from Eq. (25), are presented in

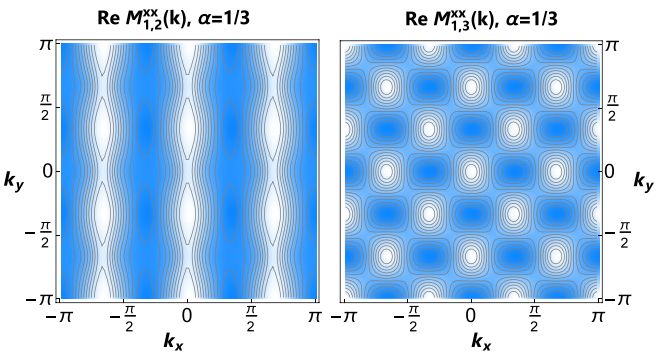

FIG. 3. Density maps of $M^{xx}_{12}(k_x,k_y)$ and $M^{xx}_{13}(k_x,k_y)$ in the case of $\alpha = 1/3$ (lighter color denotes higher values). The $\mathbf{k}$ domain spans over three Brillouin zones.

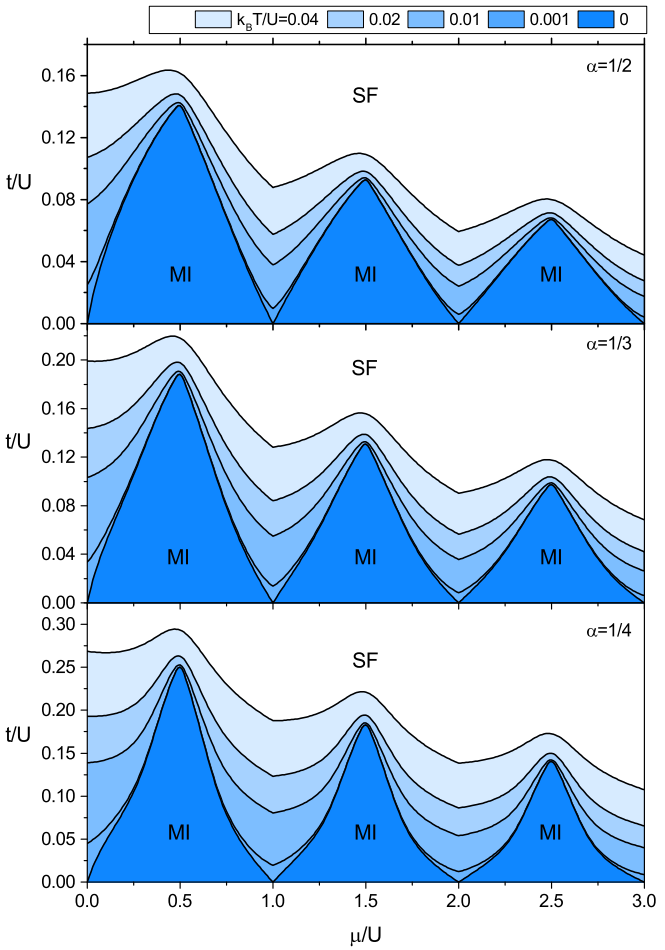

FIG. 4. Phase diagrams of superfluid to Mott insulator phase transition for three values of the flux parameter $\alpha = 1/2,\ 1/3,\ 1/4$ and for a range of values of temperature β. The Mott insulator is the ground state of the system below the critical line, while the superfluid is above. In finite temperature, the Mott insulator phase is replaced by the normal state, as the compressibility is no longer zero.

Fig. 4. The lobes of the Mott insulator phase become narrower and higher with the increasing number of bands q, which is a consequence of the band flattening [51].

Figures 5, 6, and 7 show the ground-state frequency dependence of the intra- and interband contributions to the real part of the conductivity, both in the superfluid and Mott insulator phase. As was mentioned in Sec. II C, each channel in the intraband part corresponds to the excitation of a particle-hole pair in the respective band. An example of such excitation is denoted as I in Fig. 8. In the interband case, the channels are related to excitation of a particle-hole pair, but between different bands. For example, the first sharp peak in Fig. 6 (Re $\sigma_{\text{interband}}$, superfluid) results from the excitation of a particle (hole) in the first band and hole (particle) in the second; see excitation II in Fig. 8. The Mott insulator state does not facilitate conductivity for $\omega = 0$, as can be deduced from Eq. (53). However, applying a nonstatic field of frequency greater than the energy gap $\omega_g/U = 2\sqrt{v^2(\mu/U) + \delta\lambda/U}$ allows for quasiparticle excitation and, as a result, a nonzero value of the conductivity.

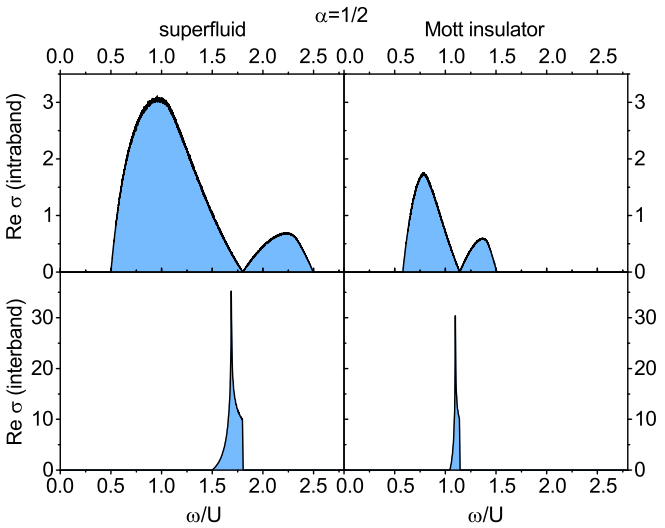

FIG. 5. Real part of the conductivity as a function of frequency of the external field for $\alpha = 1/2$. The conductivity is given in $1/\Phi_0^2$ units. The graphs were calculated for $\mu/U = 0.25$ and for $t/U = 0.18$ (superfluid) and $t/U = 0.08$ (Mott insulator).

In the superfluid state, the phase coherence facilitates the flow of the particles. This results in higher values of intraband conductivity and lower energy gap than in the MI state. Additionally, in the MI phase, the channels become narrower.

The spectral function of the system [52,53]

$$\mathscr{A}(\mathbf{k},\omega) = \sum_b \frac{1}{2\Xi_b}\left(\delta\left\{\omega - \left[\Xi_b - v\left(\frac{\mu}{U}\right)\right]\right\} + \delta\left\{\omega + \left[\Xi_b + v\left(\frac{\mu}{U}\right)\right]\right\}\right) \tag{54}$$

gives good insight into the behavior of the conductivity, especially its interband part. The spectral function dependence on wave vector and frequency is presented in Fig. 8 and shows

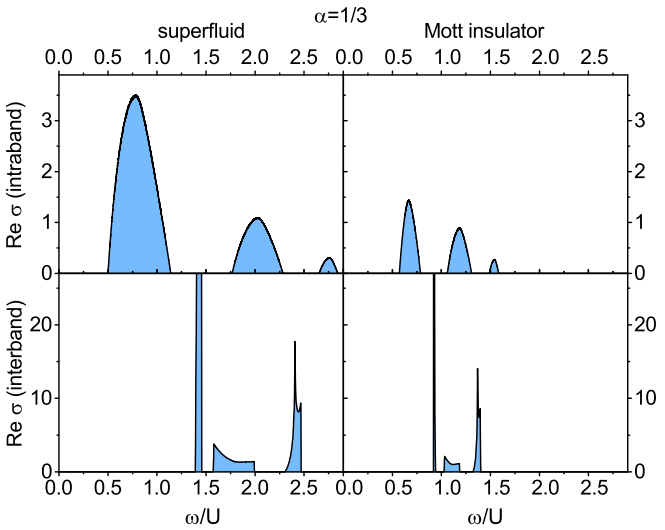

FIG. 6. Real part of the conductivity as a function of frequency of the external field for $\alpha = 1/3$, $\mu/U = 0.25$, $t/U = 0.22$ (SF), and $t/U = 0.09$ (MI) (in $1/\Phi_0^2$ units).

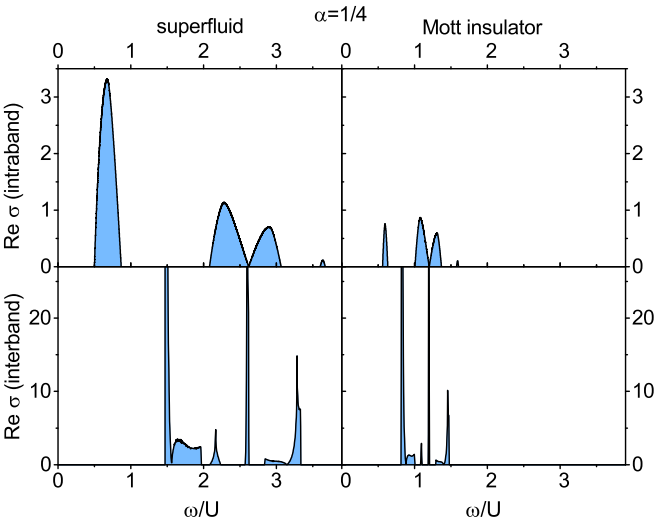

FIG. 7. Real part of the conductivity as a function of frequency of the external field for $\alpha = 1/4$, $\mu/U = 0.25$, $t/U = 0.3$ (SF), and $t/U = 0.09$ (MI) (in $1/\Phi_0^2$ units).

that the sharp, narrow peak in the interband conductivity visible in Fig. 6 between the first and the second band is a result of the first hole and the second quasiparticle band being similarly shaped (transition II in Fig. 8). Thus, there are many excitations with very similar values of frequency leading to narrow peak with large weight.

B. Finite temperature

The influence of the temperature on the intra- and interband conductivity is presented in Figs. 9 and 10 for the synthetic magnetic flux $\alpha = 1/3$. The intraband part of conductivity in

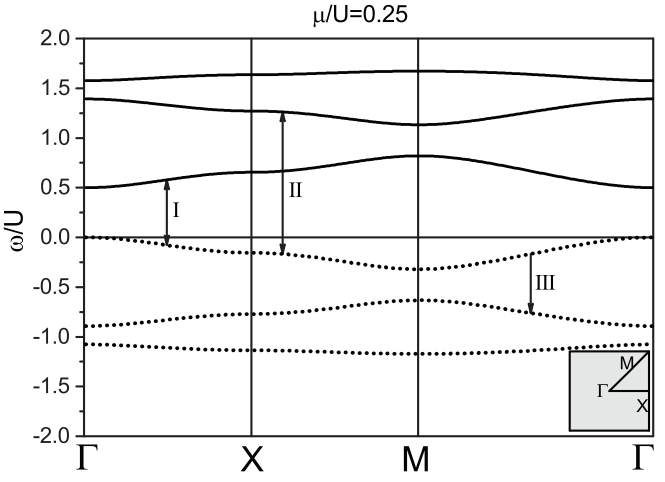

FIG. 8. Spectral function $\mathscr{A}(\mathbf{k},\omega)$ dependence on the frequency for $\alpha = 1/3$ along the lines Γ-X, X-M, and M-Γ in the reduced Brillouin zone (one third of the BZ) for $t/U = 0.22$ in the SF phase. The quasiparticle bands are drawn with solid line, while hole bands with dotted lines. Arrows denote possible excitations: I corresponds to the intraband particle-hole pair generation, II corresponds to the interband particle-hole pair, and III corresponds to the excitation of thermally excited hole.

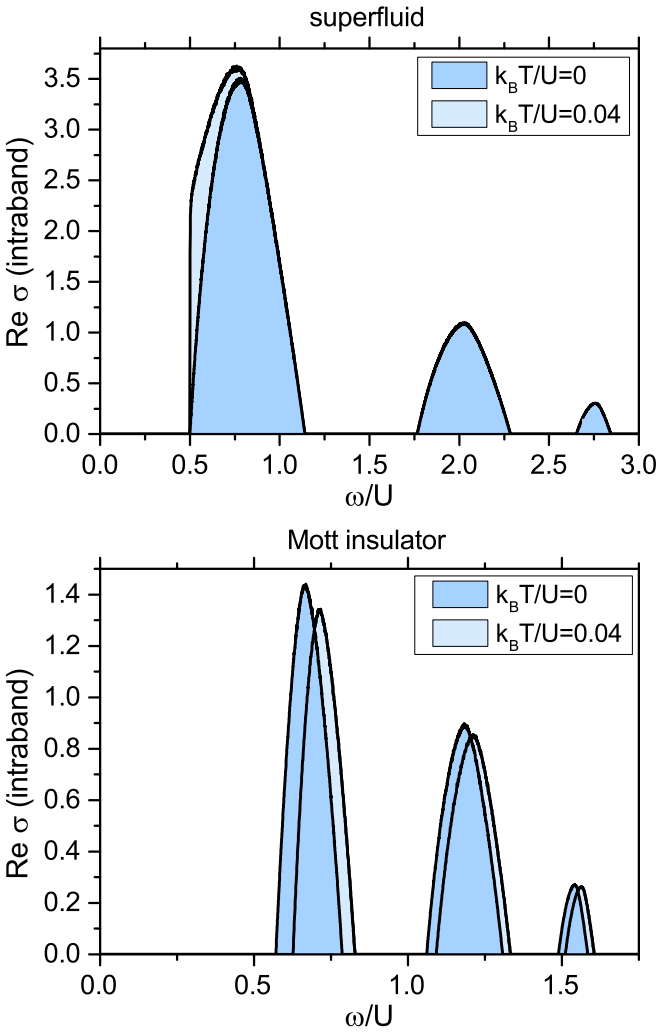

FIG. 9. Influence of the temperature on the intraband conductivity for SF ($t/U = 0.22$) and MI ($t/U = 0.09$) phases with the chemical potential $\mu/U = 0.25$.

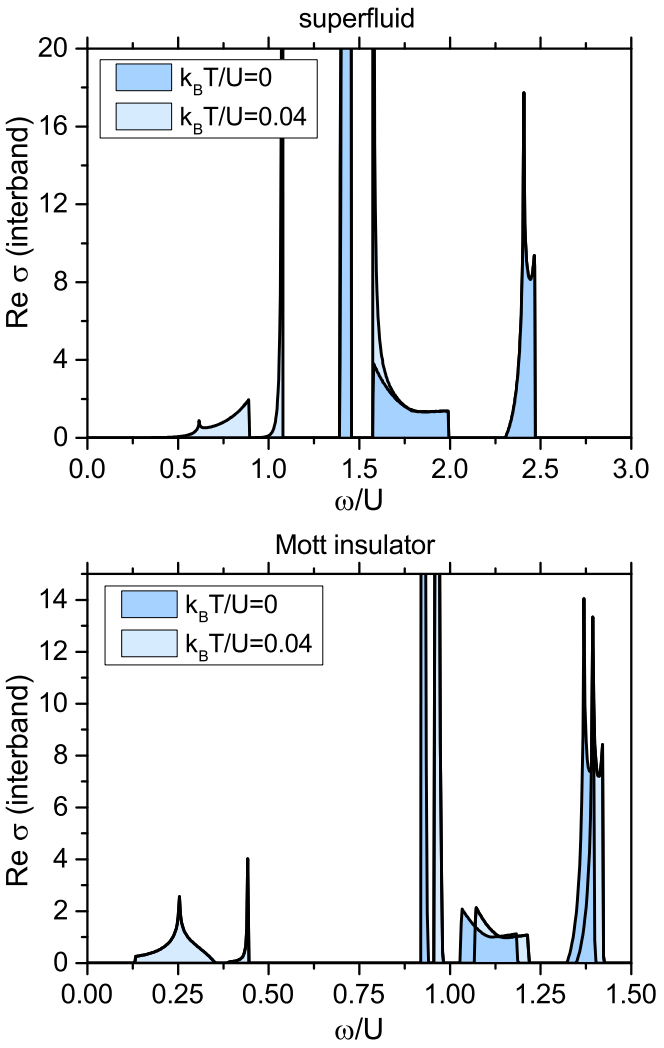

FIG. 10. Influence of the temperature on the interband conductivity for SF ($t/U = 0.22$) and MI ($t/U = 0.09$) phases with the chemical potential $\mu/U = 0.25$.

the SF phase is governed by the Bose-Einstein distribution of quasiparticles, since thermal distribution of the excitations can be rewritten as

$$f_{\pm}(\beta,\Xi_b) = \coth\left\{\frac{U\beta}{2}\left[\Xi_b \pm v\left(\frac{\mu}{U}\right)\right]\right\} = 1 + 2n_{\mathrm{BE}}\left\{U\left[\Xi_b \pm v\left(\frac{\mu}{U}\right)\right]\right\}, \quad (55)$$

where $n_{BE}(x) = 1/(e^{\beta x} - 1)$ is the Bose-Einstein distribution. Size of the gap remains constant, but the value of the conductivity near the gap edge increases as a result of quasiparticles being thermally excited. In the Mott insulator phase, the excitation gap increases with temperature. The decrease of the conductivity results from increasing $\delta\lambda$ with temperature for a chosen point on the phase diagram.

The interband part of the conductivity is modified by temperature in a similar manner as the intraband part; however, additional channels arise inside the energy gap. They are caused by the coupling of thermally excited holes or particles with the external field. This can be understood as the process of absorption of the external field quantum by a thermally excited particle (hole) and transition to a higher band; see transition III in Fig. 8. Depending on the chemical potential, the major contribution comes either from the particles or the holes with crossing points at half-integer values of μ/U. For example, for $\mu/U = 0.25$ (Fig. 10), the contribution of holes to the conductivity is dominant, while the particle channels are a few orders of magnitude smaller, thus practically negligible.

C. Universal conductivity for two-dimensional system with magnetic field

Considering strictly two-dimensional system in the zero-temperature limit, the universal value of the intraband conductivity for particle-hole symmetry points in the superfluid phase can be calculated [21,24,46]. The dispersion relation of the lowest band $\mathcal{E}_1(k_x,k_y)$ can be expanded into series around $\mathbf{k} \approx 0$. This yields

$$\mathcal{E}_1(k_x,k_y) = E_0 + a\left(k_x^2 + k_y^2\right) + \cdots, \quad (56)$$

where a is a coefficient of the series expansion. Then, the generalized density of states can be approximated for $x \approx E_0$:

$$\begin{aligned}\varrho_{xx}(x \approx E_0) &= \frac{q}{(2\pi)^2}\int_{RBZ} d^2\mathbf{k}(2ak_x)^2\delta\{x - [E_0 + a(k_x^2 + k_y^2)]\} \\ &= \frac{q}{2\pi}(x - E_0). \end{aligned} \tag{57}$$

In the presence of the (synthetic) magnetic field, the Brillouin zone consists of q reduced Brillouin zones (RBZ) with the dispersion relation being the same in each of them. Thus, in order to properly determine GDOS, the integral over RBZ must be multiplied by q. By inserting the GDOS (57) into the expression for intraband conductivity in Eq. (40) and setting $\mu/U = 1/2 + n$ $(n = 0,1,2,\dots)$ and $\delta\lambda = 0$, we arrive at the expression for the universal conductivity in the form:

$$\mathrm{Re}\,\sigma^{\mathrm{intra}}_{xx,\mathrm{reg}}(\omega \to 0) = \sigma_{\mathrm{universal}} = \frac{q\pi^2}{4\Phi_0^2}. \tag{58}$$

The universal conductivity at the particle-hole symmetry points depends only on the multiple of the degeneracy of the lowest single-particle energy state. For the systems in the magnetic field, this is equivalent to the number of magnetic subbands q. This result is in agreement with earlier papers by Cha and Girvin [54] and Sajna *et al.* [48].

IV. SUMMARY

The transport properties of ultracold bosons in optical lattices has been studied using quantum rotor approximation applied to the Bose-Hubbard model. The presence of the external magnetic field has been taken into account through Peierls substitution, effectively transforming the Bose-Hubbard Hamiltonian into Harper-Bose-Hubbard Hamiltonian and introducing the multiband energy structure of the system.

The conductivity of the system has been calculated rigorously both in the Mott insulator and superfluid phase using a quantum rotor approach. Two main contributions to the conductivity—intra- and interband—have been investigated. The former is related to the excitation of a particle-hole pair by the external field, while the latter results from the excitation of a pair; however, the particle and hole are in different bands. It is worth mentioning that the interband conductivity is heavily influenced by the relative curvature of the quasiparticle bands.

Additionally, it has been shown that in two-dimensional systems the gap vanishes at particle-hole symmetry points and the conductivity has a universal value. In the systems with the (synthetic) magnetic field, this value is multiplied by the degree of the degeneracy of the lowest single-particle energy state.

In the finite temperatures, the intraband conductivity is governed by the Bose-Einstein distribution of the quasiparticles. Additionally, for the interband part, new transport channels appear due to coupling of the thermally excited particles or holes with the external field.

The conductivity of strongly interacting lattice systems, e.g., Josephson junction arrays or optical lattices filled with bosons, was studied using various theoretical methods. However, the contribution of the interband processes had not been investigated carefully. It appears to be a significant deficiency, as it surpasses in value the intraband transport properties by at least an order of magnitude. The recent development of experimental techniques may lead to potential experimental verification of the obtained results. Multiple methods have been proposed to measure conductivity in cold-atomic systems [18,48,55,56] that can determine the current-current correlation function, which is proportional to the conductivity. An important recent proposal is a scanning gate microscope that facilitates a tightly focused laser beam that can be precisely positioned in space acting as a local perturbation [20]. By changing its position and recording subsequent variations in conductivity, a high-resolution map of transport can be retrieved. The technique has been demonstrated to work on a quantum point contact but can be in principle generalized to any cold-atomic system or extended to use multiple probes, in which case the transport should be strongly affected by interferences between atomic waves.

APPENDIX: DERIVATION OF THE EXPRESSION FOR THE CONDUCTIVITY OF A SYSTEM WITH MULTIPLE BANDS

The conductivity in terms of averages of fields $\overline{a}^c_{\mathbf{k}}(\omega_m)$, $a^c_{\mathbf{k}}(\omega_m)$ can be written as

$$\begin{aligned}\sigma_{ij}(\omega_\nu) = &-\frac{1}{N\beta^3\omega_\nu}\left(\frac{2\pi t}{\Phi_0 N_e}\right)^2 \sum_{m,\mathbf{k}}\sum_{c,d,e,f}\frac{\partial\mathcal{H}_{cd}(\mathbf{k})}{\partial k_i}\frac{\partial\mathcal{H}_{ef}(\mathbf{k})}{\partial k_j}\langle\overline{a}^c_{\mathbf{k}}(\omega_m)a^f_{\mathbf{k}}(\omega_m)\rangle\langle\overline{a}^e_{\mathbf{k}}(\omega_{\nu+m})a^d_{\mathbf{k}}(\omega_{\nu+m})\rangle \\ &+\frac{1}{N\beta^2\omega_\nu}\left(\frac{2\pi}{\Phi_0}\right)^2\frac{t}{N_e}\sum_{m,\mathbf{k}}\sum_{c,d}\frac{\partial^2\mathcal{H}_{cd}(\mathbf{k})}{\partial k_i\partial k_j}\langle\overline{a}^c_{\mathbf{k}}(\omega_m)a^d_{\mathbf{k}}(\omega_m)\rangle\end{aligned} \tag{A1}$$

with $\mathcal{H}$ being the Hamiltonian kernel in Eq. (29). The next step is the eigen decomposition of the kernel $\mathcal{H} = \mathcal{U}\mathcal{E}\mathcal{U}^{-1}$. The following properties of the unitary matrix $\mathcal{U}$ will prove useful in further derivations. The first one

$$\frac{\partial\mathcal{U}}{\partial k_i}\mathcal{U}^{-1} = -\mathcal{U}\frac{\partial\mathcal{U}^{-1}}{\partial k_i} \tag{A2}$$

results from differentiation of the formula $\mathcal{U}\mathcal{U}^{-1} = \mathbb{I}$. The second one can be obtained from the following relation:

$$\mathcal{U}^{-1}\frac{\partial}{\partial k_i}(\mathcal{H}\mathcal{U}) = \mathcal{U}^{-1}\frac{\partial\mathcal{H}}{\partial k_i}\mathcal{U} + \mathcal{U}^{-1}\mathcal{H}\frac{\partial\mathcal{U}}{\partial k_i}. \tag{A3}$$

The left-hand side of the above equation can be expanded using eigen decomposition:

$$\mathcal{U}^{-1}\frac{\partial}{\partial k_i}(\mathcal{H}\mathcal{U}) = \mathcal{U}^{-1}\frac{\partial}{\partial k_i}(\mathcal{U}\mathcal{E}\mathcal{U}^{-1}\mathcal{U}) = \mathcal{U}^{-1}\frac{\partial \mathcal{U}}{\partial k_i}\mathcal{E} + \frac{\partial \mathcal{E}}{\partial k_i}, \tag{A4}$$

similar to the right-hand side,

$$\mathcal{U}^{-1}\frac{\partial \mathcal{H}}{\partial k_i}\mathcal{U} + \mathcal{U}^{-1}\mathcal{H}\frac{\partial \mathcal{U}}{\partial k_i} = \mathcal{U}^{-1}\frac{\partial \mathcal{H}}{\partial k_i}\mathcal{U} + \mathcal{E}\mathcal{U}^{-1}\frac{\partial \mathcal{U}}{\partial k_i}. \tag{A5}$$

The whole transformed equation has now the following form:

$$\mathcal{U}^{-1}\frac{\partial \mathcal{U}}{\partial k_i}\mathcal{E} + \frac{\partial \mathcal{E}}{\partial k_i} = \mathcal{U}^{-1}\frac{\partial \mathcal{H}}{\partial k_i}\mathcal{U} + \mathcal{E}\mathcal{U}^{-1}\frac{\partial \mathcal{U}}{\partial k_i}, \tag{A6}$$

which can be rewritten as a set of equations for the matrix elements (a,d). For $a \neq d$, Eq. (A6) yields

$$\sum_b (\mathcal{U}^{-1})_{ab}\frac{\partial \mathcal{U}_{bd}}{\partial k_i}(\mathcal{E}_d - \mathcal{E}_a) = \sum_{bc}(\mathcal{U}^{-1})_{ab}\frac{\partial \mathcal{H}_{bc}}{\partial k_i}\mathcal{U}_{cd}, \tag{A7}$$

and for $a = d$

$$\frac{\partial \mathcal{E}_a}{\partial k_i} = \sum_{bc}(\mathcal{U}^{-1})_{ab}\frac{\partial \mathcal{H}_{bc}}{\partial k_i}\mathcal{U}_{ca}. \tag{A8}$$

The "paramagnetic" part of the conductivity is proportional to the quantity X, which can be transformed in the following way:

$$\begin{aligned} X &= \sum_{m,\mathbf{k}}\sum_{c,d,e,f}\frac{\partial \mathcal{H}_{cd}(\mathbf{k})}{\partial k_i}\frac{\partial \mathcal{H}_{ef}(\mathbf{k})}{\partial k_j}\langle \overline{a}^c_{\mathbf{k}}(\omega_m)a^f_{\mathbf{k}}(\omega_m)\rangle\langle \overline{a}^e_{\mathbf{k}}(\omega_{\nu+m})a^d_{\mathbf{k}}(\omega_{\nu+m})\rangle \\ &= N_e^2\beta^2|b_0|^4\sum_{m,\mathbf{k}}\sum_{b,b',c,d,e,f}\Gamma_b(\mathbf{k},\omega_m)\Gamma_{b'}(\mathbf{k},\omega_{\nu+m})(\mathcal{U}^{-1})_{bc}\frac{\partial \mathcal{H}_{cd}(\mathbf{k})}{\partial k_i}\mathcal{U}_{db'}(\mathcal{U}^{-1})_{b'e}\frac{\partial \mathcal{H}_{ef}(\mathbf{k})}{\partial k_j}\mathcal{U}_{fb}, \end{aligned} \tag{A9}$$

where the relation (33) was employed. Using the relation (A8) allows us to separate X in two terms, single band ($a = b$) and multiband ($a \neq b$):

$$X = N_e^2\beta^2|b_0|^4\sum_{m,\mathbf{k}}\sum_b \Gamma_b(\mathbf{k},\omega_m)\Gamma_b(\mathbf{k},\omega_{\nu+m})\frac{\partial \mathcal{E}_b}{\partial k_i}\frac{\partial \mathcal{E}_b}{\partial k_j} + N_e^2\beta^2|b_0|^4\sum_{m,\mathbf{k}}\sum_{b\neq b'}\Gamma_b(\mathbf{k},\omega_m)\Gamma_{b'}(\mathbf{k},\omega_{\nu+m})M^{ij}_{bb'}(\mathbf{k}), \tag{A10}$$

where $M^{ij}_{bb'}(\mathbf{k})$ was defined in Eq. (44).

The second ("diamagnetic") term in (A1), proportional to Y, requires an additional step in order to get rid of the second-order derivative over $\mathcal{H}(\mathbf{k})$. This is done by changing the sum over wave vectors into integral and performing integration by parts [21]. This yields

$$\frac{1}{N\beta^2\omega_\nu}\left(\frac{2\pi}{\Phi_0}\right)^2\frac{t}{N_e}\sum_{m,\mathbf{k}}\sum_{c,d}\frac{\partial^2 \mathcal{H}_{cd}(\mathbf{k})}{\partial k_i \partial k_j}\langle \overline{a}^c_{\mathbf{k}}(\omega_m)a^d_{\mathbf{k}}(\omega_m)\rangle = -\frac{1}{N\beta^2\omega_\nu}\left(\frac{2\pi}{\Phi_0}\right)^2\frac{t}{N_e}\sum_{m,\mathbf{k}}\sum_{c,d}\frac{\partial \mathcal{H}_{cd}}{\partial k_j}\frac{\partial}{\partial k_i}\langle \overline{a}^c_{\mathbf{k}}(\omega_m)a^d_{\mathbf{k}}(\omega_m)\rangle. \tag{A11}$$

Inserting the value of the average $\langle \overline{a}^b_{\mathbf{k}}(\omega_m)a^{b'}_{\mathbf{k}}(\omega_m)\rangle$ (33) gives

$$Y = -\sum_{m,\mathbf{k}}\sum_{c,d}\frac{\partial \mathcal{H}_{cd}}{\partial k_j}\frac{\partial}{\partial k_i}\langle \overline{a}^c_{\mathbf{k}}(\omega_m)a^d_{\mathbf{k}}(\omega_m)\rangle = -N_e\beta|b_0|^2\sum_{m,\mathbf{k}}\sum_{b,c,d}\frac{\partial \mathcal{H}_{cd}}{\partial k_j}\frac{\partial}{\partial k_i}[\mathcal{U}_{db}\Gamma_b(\mathbf{k},\omega_m)(\mathcal{U}^{-1})_{bc}]. \tag{A12}$$

This term can be separated in two parts—single and multiband—thanks to relations (A2) and (A6):

$$Y = JN_e\beta|b_0|^2\sum_{m,\mathbf{k}}\sum_b\frac{\partial \mathcal{E}_b(\mathbf{k})}{\partial k_j}\frac{\partial \mathcal{E}_b(\mathbf{k})}{\partial k_i}[\Gamma_b(\mathbf{k},\omega_m)]^2 + JN_e\beta|b_0|^2\sum_{m,\mathbf{k}}\sum_{b\neq b'}M^{ij}_{bb'}(\mathbf{k})\Gamma_b(\mathbf{k},\omega_m)\Gamma_{b'}(\mathbf{k},\omega_m). \tag{A13}$$

Combining Eq. (A1) with (A10) and (A13) gives the formula for conductivity of multiband systems

$$\begin{aligned} \sigma_{ij}(\omega_\nu) = -\frac{1}{N\beta\omega_\nu}\left(\frac{2\pi J}{\Phi_0}\right)^2\sum_{\mathbf{k},m}\Bigg\{&\sum_b\frac{\partial \mathcal{E}_b(\mathbf{k})}{\partial k_j}\frac{\partial \mathcal{E}_b(\mathbf{k})}{\partial k_i}\left[\Gamma_b(\mathbf{k},\omega_m)\Gamma_b(\mathbf{k},\omega_{m+\nu}) - \Gamma_b^2(\mathbf{k},\omega_m)\right] \\ &+\sum_{b\neq b'}M^{ij}_{bb'}(\mathbf{k})[\Gamma_b(\mathbf{k},\omega_m)\Gamma_{b'}(\mathbf{k},\omega_{m+\nu}) - \Gamma_b(\mathbf{k},\omega_m)\Gamma_{b'}(\mathbf{k},\omega_m)]\Bigg\}. \end{aligned} \tag{A14}$$

[1] J.-P. Brantut, J. Meineke, D. Stadler, S. Krinner, and T. Esslinger, Science **337**, 1069 (2012).
[2] S. Krinner, D. Stadler, D. Husmann, J.-P. Brantut, and T. Esslinger, Nature (London) **517**, 64 (2015).
[3] J.-P. Brantut, C. Greiner, J. Meineke, D. Stadler, S. Krinner, C. Kollath, T. Esslinger, and A. Georges, Science **342**, 713 (2013).
[4] S. Krinner, D. Stadler, J. Meineke, J.-P. Brantut, and T. Esslinger, Phys. Rev. Lett. **110**, 100601 (2013).
[5] D. Stadler, S. Krinner, J. Meineke, J.-P. Brantut, and T. Esslinger, Nature (London) **491**, 736 (2012).
[6] C.-C. Chien, S. Peotta, and M. Di Ventra, Nat. Phys. **11**, 998 (2015).
[7] D. Husmann, S. Uchino, S. Krinner, M. Lebrat, T. Giamarchi, T. Esslinger, and J.-P. Brantut, Science **350**, 1498 (2015).
[8] S. Krinner, M. Lebrat, D. Husmann, C. Greiner, J.-P. Brantut, and T. Esslinger, Proc. Natl. Acad. Sci. USA **113**, 8144 (2016).
[9] M. Kanász-Nagy, L. Glazman, T. Esslinger, and E. A. Demler, Phys. Rev. Lett. **117**, 255302 (2016).
[10] M. Aidelsburger, M. Atala, M. Lohse, J. T. Barreiro, B. Paredes, and I. Bloch, Phys. Rev. Lett. **111**, 185301 (2013).
[11] H. Miyake, G. A. Siviloglou, C. J. Kennedy, W. C. Burton, and W. Ketterle, Phys. Rev. Lett. **111**, 185302 (2013).
[12] M. Aidelsburger, M. Lohse, C. Schweizer, M. Atala, J. T. Barreiro, S. Nascimbène, N. R. Cooper, I. Bloch, and N. Goldman, Nat. Phys. **11**, 162 (2014).
[13] M. Atala, M. Aidelsburger, M. Lohse, J. T. Barreiro, B. Paredes, and I. Bloch, Nat. Phys. **10**, 588 (2014).
[14] M. Weinberg, C. Ölschläger, C. Sträter, S. Prelle, A. Eckardt, K. Sengstock, and J. Simonet, Phys. Rev. A **92**, 043621 (2015).
[15] C. J. Kennedy, W. C. Burton, W. C. Chung, and W. Ketterle, Nat. Phys. **11**, 859 (2015).
[16] S. Peotta, C.-C. Chien, and M. Di Ventra, Phys. Rev. A **90**, 053615 (2014).
[17] W. S. Bakr, J. I. Gillen, A. Peng, S. Fölling, and M. Greiner, Nature (London) **462**, 74 (2009).
[18] S. Keßler and F. Marquardt, Phys. Rev. A **89**, 061601 (2014).
[19] M. F. Parsons, A. Mazurenko, C. S. Chiu, G. Ji, D. Greif, and M. Greiner, Science **353**, 1253 (2016).
[20] S. Häusler, S. Nakajima, M. Lebrat, D. Husmann, S. Krinner, T. Esslinger, and J.-P. Brantut, Phys. Rev. Lett. **119**, 030403 (2017).
[21] A. P. Kampf and G. T. Zimanyi, Phys. Rev. B **47**, 279 (1993).
[22] I. S. Beloborodov, Y. V. Fominov, A. V. Lopatin, and V. M. Vinokur, Phys. Rev. B **74**, 014502 (2006).
[23] D. Domínguez and J. V. José, Phys. Rev. B **53**, 11692 (1996).
[24] A. van Otterlo, K.-H. Wagenblast, R. Fazio, and G. Schön, Phys. Rev. B **48**, 3316 (1993).
[25] T. K. Kopeć and J. V. José, Phys. Rev. B **60**, 7473 (1999).
[26] I. Bloch, J. Dalibard, and W. Zwerger, Rev. Mod. Phys. **80**, 885 (2008).
[27] M. P. A. Fisher, P. B. Weichman, G. Grinstein, and D. S. Fisher, Phys. Rev. B **40**, 546 (1989).
[28] D. Jaksch, C. Bruder, J. I. Cirac, C. W. Gardiner, and P. Zoller, Phys. Rev. Lett. **81**, 3108 (1998).
[29] P. G. Harper, Proc. Phys. Soc. A **68**, 874 (1955).
[30] D. R. Hofstadter, Phys. Rev. B **14**, 2239 (1976).
[31] T. P. Polak and T. K. Kopeć, Phys. Rev. B **76**, 094503 (2007).
[32] S. Sachdev, *Quantum Phase Transitions* (Cambridge University Press, Cambridge, UK, 2011).
[33] F. P. Mancini, P. Sodano, and A. Trombettoni, Phys. Rev. B **67**, 014518 (2003).
[34] H. Chamati, E. S. Pisanova, and N. S. Tonchev, Phys. Rev. B **57**, 5798 (1998).
[35] T. A. Zaleski and T. K. Kopeć, Phys. Rev. B **62**, 9059 (2000).
[36] T. K. Kopeć, Phys. Rev. B **70**, 054518 (2004).
[37] J. Ye, S. Sachdev, and N. Read, Phys. Rev. Lett. **70**, 4011 (1993).
[38] T. A. Zaleski and T. K. Kopeć, Phys. Rev. A **84**, 053613 (2011).
[39] T. P. Polak and T. A. Zaleski, Phys. Rev. A **87**, 033614 (2013).
[40] A. L. Fetter and J. D. Walecka, *Quantum Theory of Many-Particle Systems* (McGraw-Hill, San Francisco, 1971).
[41] H. Kleinert, *Path Integrals in Quantum Mechanics, Statistics, Polymer Physics, and Financial Markets* (World Scientific, Singapore, 2006).
[42] S. Florens and A. Georges, Phys. Rev. B **66**, 165111 (2002).
[43] D. Pesin and L. Balents, Nat. Phys. **6**, 376 (2010).
[44] T. Vojta, Phys. Rev. B **53**, 710 (1996).
[45] T. M. Nieuwenhuizen, Phys. Rev. Lett. **74**, 4293 (1995).
[46] M.-C. Cha, M. P. A. Fisher, S. M. Girvin, M. Wallin, and A. P. Young, Phys. Rev. B **44**, 6883 (1991).
[47] J. Wu and P. Phillips, Phys. Rev. B **73**, 214507 (2006).
[48] A. S. Sajna, T. P. Polak, and R. Micnas, Phys. Rev. A **89**, 023631 (2014).
[49] N. D. Mermin and H. Wagner, Phys. Rev. Lett. **17**, 1133 (1966).
[50] J. Struck, M. Weinberg, C. Ölschläger, P. Windpassinger, J. Simonet, K. Sengstock, R. Höppner, P. Hauke, A. Eckardt, M. Lewenstein *et al.*, Nat. Phys. **9**, 738 (2013).
[51] B. Grygiel, K. Patucha, and T. A. Zaleski, Phys. Rev. A **93**, 053607 (2016).
[52] T. A. Zaleski, J. Phys. B: At. Mol. Opt. Phys. **45**, 145303 (2012).
[53] T. A. Zaleski and T. K. Kopeć, Physica B **433**, 37 (2014).
[54] M.-C. Cha and S. M. Girvin, Phys. Rev. B **49**, 9794 (1994).
[55] A. Tokuno and T. Giamarchi, Phys. Rev. Lett. **106**, 205301 (2011).
[56] A. S. Sajna and T. P. Polak, Phys. Rev. A **90**, 043603 (2014).